Chirality-Regulated Spin Polarization of Perovskite Nanoplates for Photocatalytic CO_2 Reduction

The manipulation of spin-polarized electrons through chirality-regulated perovskite nanocrystals significantly enhances photocatalytic CO_2 reduction efficiency and highlights their strong potential for future solar-to-fuel conversion applications.

Artificial photosynthesis, which relies on solar-driven CO_2 reduction to generate high-value fuels, has recently attracted considerable attention as a promising approach to addressing both climate change and the global energy crisis. Among various strategies, photocatalytic CO_2 reduction has emerged as an especially appealing route, enabling the conversion of CO_2 into useful fuels and chemical feedstocks using renewable energy.[1] Chun-Wei Chen (National Taiwan University) and his collaborators demonstrate that photocatalytic CO_2 reduction efficiency can be markedly enhanced through chirality-regulated spin polarization in $CsPbBr_3$ perovskite nanocrystals.[2] Incorporating chiral molecules into layered perovskites provides an effective pathway to induce spin polarization, which in turn significantly boosts photocatalytic activity. Motivated by these insights, Chen and Chun-Jen Su (NSRRC) developed chirality-regulated perovskite thin films by introducing chiral organic molecules (MBA·Br) into all-inorganic $CsPbBr_3$ perovskite nanoplates (NPLs). This approach produces (R)- and (S)-two-dimensional (2D) Ruddlesden–Popper perovskite (RPP)/NPL hybrid structures. Within this hybrid configuration, the chiral 2D RPP domains impart strong chiroptical responses that facilitate the generation of spin-polarized electrons. As a result, chirality-induced spin polarization in these 2D RPP/NPL hybrid perovskite thin films effectively suppresses charge-carrier recombination, ultimately leading to a substantial enhancement in photocatalytic CO_2 reduction (CO_2RR) performance.

To elucidate the layered crystal structures of the synthesized materials, 2D grazing-incidence wide-angle X-ray scattering (2D-GIWAXS) measurements were conducted at the **TLS 23A1** beamline at the NSRRC. This technique enables comprehensive examination of crystallinity, phase composition, and lattice orientation in thin-film perovskite systems. As shown in **Fig. 1(d)**, the GIWAXS pattern of pristine $CsPbBr_3$ perovskite NPLs exhibits distinct

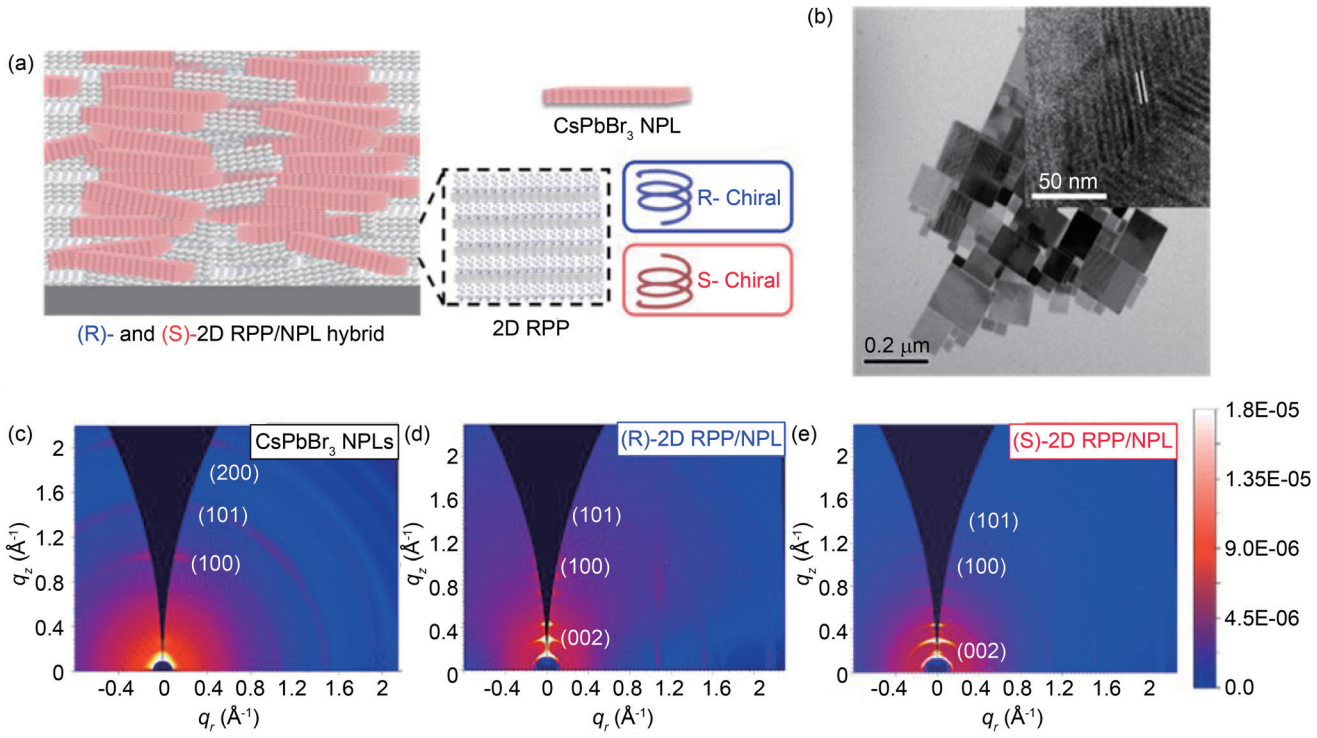

Fig. 1: Morphology and structural characterization of $CsPbBr_3$ perovskite NPLs, (R)-2D RPP/NPL, and (S)-2D RPP/NPL. (a) Schematic diagram of the (R)- and (S)-2D RPP/NPL hybrid perovskite thin films. (b) TEM image showing the morphology of $CsPbBr_3$ NPLs; the inset presents an HRTEM cross-sectional image of $CsPbBr_3$ NPLs. The 2D GIWAXS patterns of (c) $CsPbBr_3$ NPLs, (d) (R)-2D RPP/NPL, and (e) (S)-2D RPP/NPL. [Reproduced from Ref. 1]

diffraction features corresponding to the (100), (101), and (200) lattice planes. These peaks are characteristic signatures of the three-dimensional (3D) perovskite crystal structure, indicating that the $CsPbBr_3$ NPLs retain a crystallographic framework comparable to bulk 3D $CsPbBr_3$ perovskites. The results also confirm that the NPLs possess a highly anisotropic and layered morphology, with an ultrathin thickness of only a few nanometers, consistent with their nanoplate-like geometry. By contrast, the GIWAXS patterns of the (R)- and (S)-2D RPP/NPL hybrid $CsPbBr_3$ perovskite thin films—shown in **Figs. 1(d) and 1(e)**, respectively—display pronounced low scattering wavevector ($q < 1$ Å^{-1}) features. These low-q reflections are hallmarks of a 2D organic–inorganic hybrid RPP phase, confirming the incorporation of layered perovskite domains within the hybrid films. Notably, the (002) diffraction peak of the 2D RPP structure appears at $q = 0.16$ Å^{-1}, corresponding to an interlayer spacing of approximately 3.9 nm. This value closely matches the structural parameters of the $(MBA)_2Cs_3Pb_4Br_{13}$ perovskite (n = 4) phase. After accounting for the thickness of the organic chiral ligands, the thickness of the inorganic perovskite slabs is estimated to be ~3 nm, which is in good agreement with the cross-sectional High-Resolution Transmission Electron Microscopy (HRTEM) observations of $CsPbBr_3$ NPLs shown in the inset of **Fig. 1(b)**.

Furthermore, subtle but identifiable diffraction features at $q \approx 1.08$ Å^{-1} and 1.50 Å^{-1} in the hybrid films indicate the coexistence of 3D-like structural motifs within the predominantly 2D RPP–NPL architecture. These mixed-phase signatures suggest that the hybrid films consist of chiral 2D RPP layers embedded within or interfaced with the non-chiral $CsPbBr_3$ NPL matrix, forming a structurally integrated composite. Taken together, the GIWAXS results verify that our two-step synthesis protocol successfully produces both (R)- and (S)-2D RPP/NPL hybrid perovskite thin films with well-defined layered structures. Importantly, the embedded chiral RPP domains serve as key structural components responsible for transferring molecular chirality into the inorganic lattice, thereby generating spin-polarized charge carriers within the non-chiral perovskite NPL framework.

Circular dichroism (CD) and circularly polarized luminescence (CPL) reveal distinct chiroptical responses within the absorption and emission bands of the NPLs, indicating chirality transfer from the organic ligands to the inorganic layers (**Fig. 2**). Pristine $CsPbBr_3$ films show no CD signals, whereas hybrid R/S-2D RPP/NPL samples display pronounced signals, consistent with chiral-induced excitonic coupling within the metal-halide planes.

Under illumination, these chiral hybrid films show significantly improved photocatalytic CO_2RR performance (**Fig. 3**). The (R)- and (S)-2D RPP/NPL films achieve CO production rates of 45.5 and 30.6 μmol g^{-1}, respectively, substantially higher than the 15.1 μmol g^{-1} of pristine $CsPbBr_3$. Applying a 0.3 T external magnetic field further increases the CO yield to 75.3 and 49.3 μmol g^{-1},

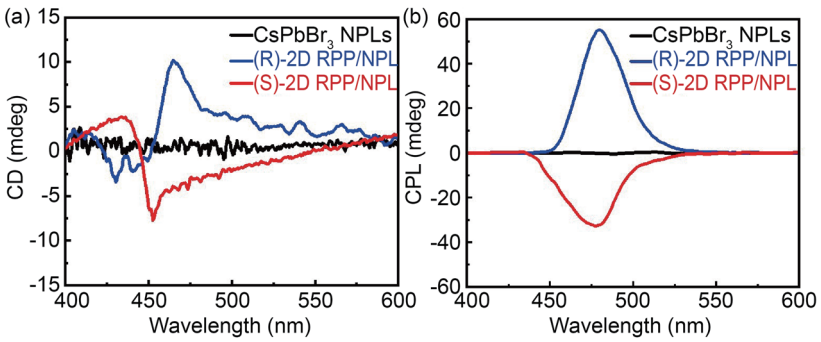

Fig. 2: (a) CD spectra of $CsPbBr_3$ NPLs, (R)-2D RPP/NPL, and (S)-2D RPP/NPL prepared using the two-step synthesis process. (b) CPL spectra of $CsPbBr_3$ NPLs, (R)-2D RPP/NPL, and (S)-2D RPP/NPL. [Reproduced from Ref. 1]

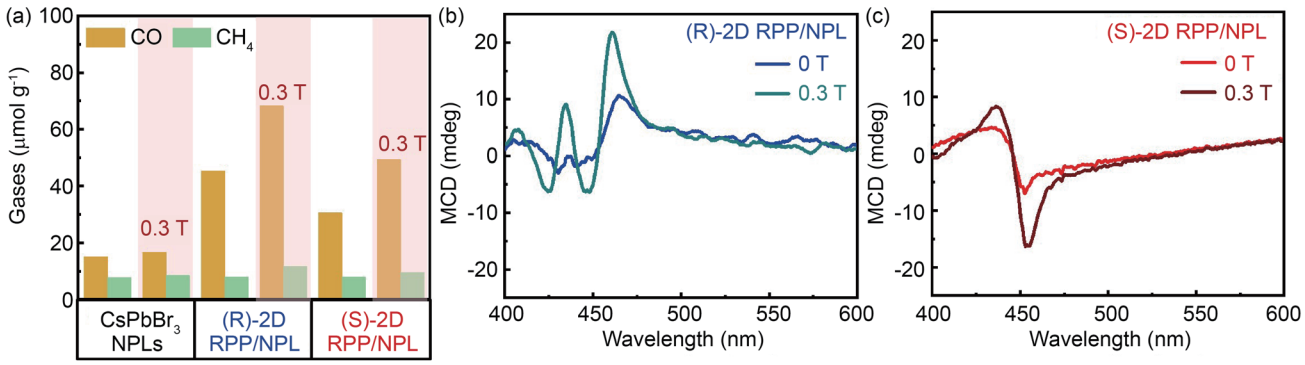

Fig. 3: The photocatalytic performance and MCD spectra of $CsPbBr_3$ NPLs, (R)-2D RPP/NPL, and (S)-2D RPP/NPL were evaluated with and without an external magnetic field (0.3 T). (a) Photocatalytic yield measurements for $CsPbBr_3$ NPLs, (R)-2D RPP/NPL, and (S)-2D RPP/NPL were conducted under irradiation for 6 hours, both with and without an external magnetic field (0 and 0.3 T). (b) and (c) show the MCD spectra of (R)-2D RPP/NPL and (S)-2D RPP/NPL, respectively, under both conditions (0 and 0.3 T). [Reproduced from Ref. 1]

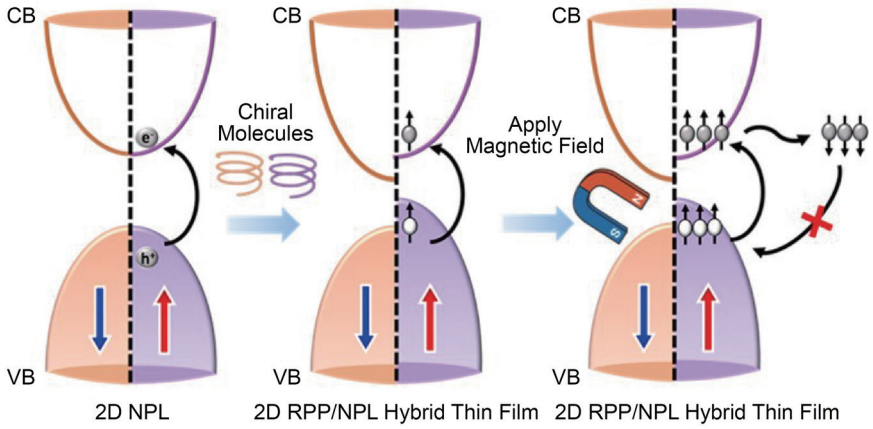

Fig. 4: Schematic illustration of the extended photoexcited carrier lifetime caused by electron spin polarization under an external magnetic field in chiral 2D RPP/NPL. [Reproduced from Ref. 1]

representing over a 60% improvement compared to zero-field conditions. This enhancement correlates with Zeeman splitting-induced amplification of spin-polarized electronic states, as confirmed by magnetic circular dichroism (MCD).

Figure 4 shows how spin-polarization control in chirality-regulated 2D RPP/NPL hybrid perovskite films enhances photocatalytic CO_2RR. In both (R)- and (S)-2D RPP/NPL hybrids, chirality transfer from chiral molecules induces spin-polarized band structures with asymmetric spin-up and spin-down density of states (DOS), unlike pristine $CsPbBr_3$ NPLs, which have symmetric DOS. Under illumination, photoexcited spin-polarized electrons typically undergo spin relaxation due to strong spin–orbit coupling and hyperfine interactions; however, carrier recombination is suppressed because spin-polarized holes of matching orientation in the valence band are limited. This extends carrier lifetimes and improves CO_2RR efficiency in the chiral hybrids. An external magnetic field introduces additional Zeeman splitting, increasing spin-polarized carrier populations and further prolonging lifetimes. This mechanism demonstrates the link between spin polarization control in chirality-regulated 2D RPP/NPL hybrid perovskite thin films and enhanced photocatalytic CO_2RR.

This work demonstrates that chirality-induced spin polarization effectively suppresses recombination and promotes charge transfer in perovskite photocatalysts. Coupling this approach with external magnetic fields further enhances CO_2-to-fuel conversion efficiency, suggesting a promising direction for high-performance solar-to-fuel platforms. (Reported by Chun-Wei Chen, National Taiwan University)

This report features the work of Chun-Wei Chen and his collaborators published in J. Am. Chem. Soc. ***147****, 40347 (2025).*

TLS 23A1 Small/Wide Angle X-ray Scattering

- GIWAXS
- Materials Science, Chemistry, Material Structure

References

1. C.-C. Lin, S.-K. Huang, W.-N. Tseng, C.-J. Su, C.-C. Huang, C.-Y. Huang, C.-Y. Yu, M.-H. Lai, J.-Y. Sun, Y.-C. Chao, H.-S. Hsu, C.-W. Luo, Y.-M. Chang, C.-C. Chen, C.-W. Chen, J. Am. Chem. Soc. **147**, 40347 (2025).
2. C.-C. Lin, T.-R. Liu, S.-R. Lin, K. M. Boopathi, C.-H. Chiang, W.-Y. Tzeng, W.-H. C. Chien, H.-S. Hsu, C.-W. Luo, H.-Y. Tsai, H.-A. Chen, P.-C. Kuo, J. Shiue, J.-W. Chiou, W.-F. Pong, C.-C. Chen, C.-W. Chen, J. Am. Chem. Soc. **144**, 15718 (2022).